Architectures for Detecting Real-time Multiple Multi-stage Network Attacks Using Hidden Markov Model

Tawfeeq Shawly, *Student, IEEE*, Ali Elghariani, *Member, IEEE*, Jason Kobes, *Member, IEEE*, and Arif Ghafoor, *Fellow, IEEE*

Abstract

With the growing Cyber threats, the need to develop high assurance Cyber systems is becoming increasingly important. The objective of this paper is to address the challenges of modeling and detecting sophisticated and diversified network attacks. Using one of the important statistical machine learning (ML) techniques, Hidden Markov Models (HMM), we develop two architectures that can detect and track in real-time the progress of these organized attacks. These architectures are based on developing a database of HMM templates and exhibit varying performance and complexity. For performance evaluation, in the presence of multiple multi-stage attack scenarios, various metrics are proposed which include (1) attack risk probability, (2) detection error rate, and (3) the number of correctly detected stages. Extensive simulation experiments are used based on the DARPA2000 dataset to demonstrate the efficacy of the proposed architectures.

Index Terms

Cyber systems, network security, intrusion detection, Hidden Markov Model, interleaved attacks.

I. Introduction

Large organizations face a daunting challenge in providing security to their Cyber-based systems. Modern Cyber-based infrastructures typically consist of a large number of interdependent systems and exhibit increasing reliance on the security of such systems. In the present threat landscape, network attacks have become more advanced, sophisticated and diversified, and the rapid pace of coordinated Cyber security crimes has witnessed a massive growth over the past several years. Cyber attacks can affect and downgrade functionalities and missions of critical

infrastructures [1], [2]. For instance, in December 2015, hackers were able to successfully compromise information systems of three energy distribution companies in Ukraine and temporarily disrupted power supply to consumers [3]. Another recent incident was in May 2017 where the "WannaCry" ransomware attack was detected after it locked up over 200,000 servers in more than 150 countries [4]. A month later, another version of the same attack caused outages of most of the government websites and several companies in Ukraine. Later on, this attack spread worldwide [5].

With the explosive growth of Cyber threats, there is a dire need to develop high assurance and resilient Cyber-based systems. One of the most important requirements for high assurance systems is to develop advanced and sophisticated attack detection and prediction systems [1].

Security reports reveal that, over time, the type of network intrusion has transformed from the original Trojan horses and viruses into more complex attacks comprising of myriad of individual attacks. These attacks follow a series of long term steps and actions, and are called multi-stage attacks and, therefore, are hard to predict [6]–[8]. In these attacks, an intruder launches several actions, which may not be performed simultaneously, but are correlated in the sense that each action is part of the execution of previous ones and are aimed at a specific target. The detection of multi-stage attacks poses a daunting challenge to the existing threat detection techniques [1]. This challenge is exacerbated if multiple of these attacks are launched simultaneously in the network originated by a single or multiple attackers [8], [9].

In the past, various approaches have been proposed to address intrusion prediction and detection challenges related to multi-stage attacks. These approaches can, in general, be categorized as correlation based techniques [10]–[12] or machine learning (ML) based techniques. Examples of ML techniques include Hidden Markov Models, Bayesian Networks, Clustering and Neural Networks [2], [13]–[15]. Correlation-based techniques, based on cause and effect relationship, mainly utilize attack-graphs in searching the possible stages of the attack [16]–[21]. For example, the work in [17] focuses on the causal relationships between attack phases on the basis of security information. The work in [18] assesses network security through mining and restoring the attack paths within an attack graph. A causal relations graph presented in [19], contains the low-level attack patterns in the form of their prerequisites and consequences. In that approach, during the correlation phase, new search is performed upon the arrival of a new alert. Several other techniques use similar ideas for analyzing attack scenarios from security alerts [20], [21]. However, most of these approaches depend on correlation rules in conjunction with the domain

knowledge. Due to increased computational complexity in detecting real time attacks, these techniques pose a limitation.

In the category of ML technique, HMM is a leading approach in intrusion detection and prediction of multi-stages attacks [22]–[31]. In this approach, stages of an attack are modeled as states of the HMM. The existing HMM based detection systems, however, are primarily focused on single multi-stage attacks. HMM is considered the most suitable detection techniques for such attacks for several reasons [22]. First, it has a tractable mathematical formalism in terms of analyzing input-output relationships, and generating transition probability matrices based on training dataset. Second, because it is specialized to deal with sequential data by exploiting transition probability between states, it can track the progress of a multi-stage attack.

Existing approaches address only a single multi-stage attack. The problem of detecting multiple interleaved multi-stage attacks has not been addressed in the literature. Several challenges are faced for detecting interleaved attacks which include: (1) how to model each multi-stage attack in terms of HMM states in the presence of mixed observations, (2) how to detect a multi-stage attack when an attacker(s) performs interleaved attacks with the intention to hide an attack, (3) since there is no standard public dataset available that provides interleaved traffic from simultaneous multiple attacks, generating this type of datasets poses a challenge, (4) design an efficient architecture that detects and tracks the progress of multiple simultaneous attacks, and (5) how to accurately quantify and measure the detection performance of such an architecture.

To address the above challenges, in this paper, we propose two architectures based on HMM formalism. The proposed architectures exhibit varying detection performance and processing complexities. The architectures can detect the occurrence of multiple organized attacks and provide insights about the dynamics of these attacks such as identifying which attack is progressing and which one is idle at any point of time; how fast or slow each attack is progressing; and in which security state each attack is in at a certain time. Knowledge of these insights can assist in designing effective response mechanisms that can mitigate security risk to the network [1], [32]. The design of the first proposed architecture relies on modifying HMM model parameters to detect multiple multi-stage attacks in the presence of mixed alerts. While on the other hand, the second proposed architecture relies on de-interleaving mixed alerts from different attacks prior to the HMM processing subsystem. We compare the two architectures in terms of their detection performance and design complexity.

The remainder of this paper is organized as follows. We introduce the system model in Section

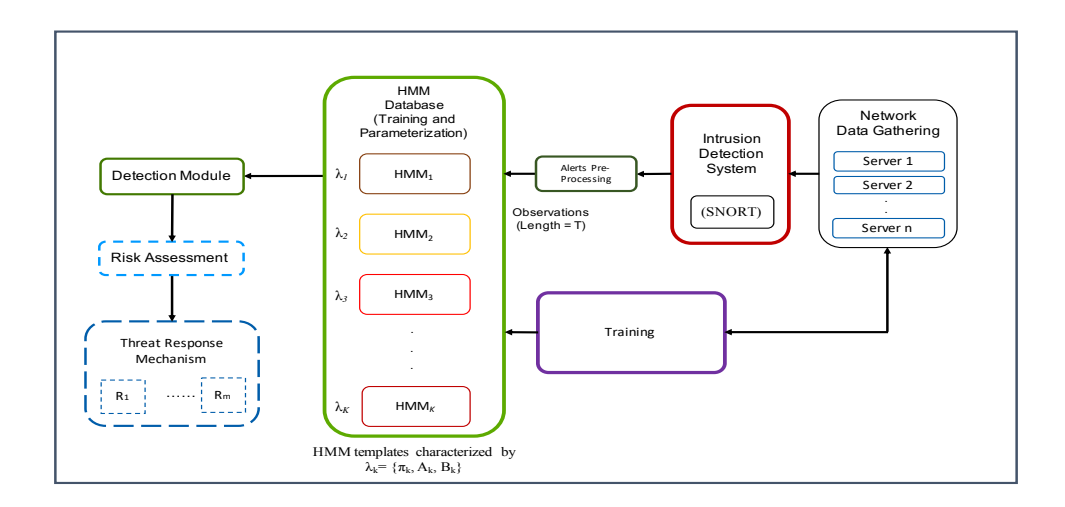


Fig. 1: A generic architecture for multiple multi-stage attack detection using an HMM database

II. We present the proposed architectures in Section III and evaluation and performance measures in Section IV. We conclude the paper in Section V.

II. SYSTEM MODEL AND ARCHITECTURE

In order to detect multiple multi-stage attacks, say K attacks, one can generalize the existing single attack architecture by building a database of K HMM templates. In Fig. 1, we present a generic architecture for the threat detection process that uses such a database. Here, each HMM-based template, is designed to detect a specific type of multi-stage attack. The goal of this architecture is to detect K multi-step attacks originated from a single or multiple attackers. Note, each of the K HMM templates is trained for detecting an individual multi-step attack. Each template encompasses the HMM structure including the transition probability matrix and a number of states [33].

The second major component of this architecture is the intrusion detection system (IDS), (e.g., SNORT software [34], [35]), which generates the attack related alerts in real time from the network traffic according to a predefined set of rules. Typically, an IDS generates a stream of alerts which are temporally ordered based on their timestamps. The online processing of this stream of alerts can potentially require a large amount of memory [36]. The selection of IDS rules can help in reducing the large volume of alerts, as well as can reduce false positives. The interleaved alerts generated by SNORT can belong to one or multiple attacks. These alerts can be preprocessed to generate observations in a suitable format that can be forwarded to the HMM

database. Based on the information from SNORT, preprocessing module can assign different severity levels for the incoming alerts. The higher the level is, the more severe the alert is, which indicates that an ongoing multi-stage attack is progressing towards an advanced stage. In this paper, the incoming alerts to the system are grouped to form an observation sequence of length T. Note, the risk of progressing multi-stage attacks can be assessed in real time by the risk assessment component and prioritized response actions can be taken based on detected states and the risk of the active attacks [1].

In the following, we present a preliminary discussion about HMM formalism and subsequently, in Section III, we use this model to build the proposed architectures.

A. Hidden Markov Model Description

An HMM is a doubly stochastic process [33] with an underlying stochastic process that is hidden, and can only be observed through another set of stochastic processes that produce the sequence of observed symbols. The observation process corresponds to alerts generated by the IDS. In this section, we provide mathematical preliminaries for the discrete HMM in the context of multiple multi-stage attacks. Consider that each attack is modeled using a distinct HMM model λ_k that encompasses all the following parameters,

$$\lambda_k = \{S_k, V_k, A_k, B_k, \pi_k\}, \quad k = 1, 2, \dots, K$$
 (1)

where $S_k = \{s_{1_k}, \ldots, s_{n_k}, \ldots, s_{N_k}\}$, s_{n_k} represents State n of Attack k, and N_k is the number of states in Attack k. Note, for multiple attacks, different attacks can have different values of N. In this paper, for simplicity of HMM computations, we assume that ongoing multistage attacks in the network can be modeled with the same number of security states. $V_k = \{v_{1_k}, \ldots, v_{m_k}, \ldots, v_{M_k}\}$ represents distinct observation symbols set for Attack k, where M_k is the total number of distinct observations for Attack k. In our model, we consider both the cases of $V_i \cap V_j = \phi$ and $V_i \cap V_j \neq \phi$, for $j \neq i$, and $j, i = 1, 2, \ldots, K$. That is, any two multistage attacks can have the same set of observations. A_k represents the state transition probability matrix of Attack k with dimension $N_k \times N_k$. Each element in this matrix, a_{ij} , represents the state transition probability form state i to state j as follows:

$$a_{ij} = P(x_{t+1} = s_j | x_t = s_i),$$

 $1 \le i \le N_k, \ 1 \le j \le N_k, \ x_t \in S_k$

 B_k is the observation emission probability matrix with dimension $N_k \times M_k$. The emission probability of the m^{th} observation of state j is represented by $b_j(m)$, as follows:

$$b_j(m) = Pr(o_t = v_m | x_t = s_j),$$

$$1 \le j \le N_k, \ 1 \le m \le M_k$$

Initial probability distribution vector (π) represents initial states probabilities of the HMM states with $\pi_i = Pr(x_1 = s_i)$, $1 \le i \le N$. The observation sequence (O) of length T for HMM is represented as $O = \{o_1, o_2, \ldots, o_t, \ldots, o_T\}$ where $o_t \in V_k$. As indicated in [33], HMM can deal with three main problems which are, the evaluation, hidden state decoding, and model training. Note, all of these problems need to be addressed for designing our architectures.

1) HMM model Type: An important consideration that needs to be taken into account when choosing HMM for an application, is the type of the model. There are mainly two types of HMM in terms of state transition diagram. One is called ergodic HMM or fully connected HMM, in which every state of the model can be reached from every other state in a single step [33]. The other type of HMM is the left-right HMM which has the property that as the time progresses, the state number increases, i.e., state transition proceeds from left to right and there is no return transition. This type of modeling puts a constraint on the state probability matrix such that:

$$a_{ij} = 0, \quad j < i$$

The left-right HMM model is suitable for the type of applications where states change over time. This applies to the problem of a multi-stage attack that progresses over time to reach the goal of compromising a certain target. Even though the attacker sometimes may perform actions that are supposed to lead to lower security states from the current state for reasons depend on the type of attack, the left-right HMM does not allow transition to a lower state. Therefore, one of the proposed architectures is modeled using a modified HMM model where right-left transitions are allowed for a specific state as discussed in Section III-A.

2) The Number of HMM States: The selection of the optimum number of states for each HMM template is a challenge and there is no simple theoretical answer to how, in general, this parameter can be selected [33]. This parameter depends on the type of application. In this paper, we model the number of HMM states to be similar to the number of stages of the multi-stage attack. The justification is that the closer the number of states to the number of stages in the multi-stage attack, the better details can be provided about the progress of the attack and thus, it can lead to the development of more effective response mechanism.

3) HMM Model Training: The most important part of the HMM database in the generic architecture of the detection system (Fig. 1) is the parameterization of HMMs in terms of determining both A_k and B_k matrices in (1) to maximize probability $Pr(O|\lambda_k)$ for each multistage attack. There are several unsupervised training algorithms, such as Baum-Welch (BW) and Expectation Maximization (EM) [33]. In this paper, we use BW training algorithm as it is the most widely used algorithm and it is a special case of the EM method applied to HMM training [33]. Furthermore, since we have a limited availability of public datasets with multiple multistage attacks, we train HMMs with a small number of training data points, although practically the larger the number of training data points the better the model is, and thus the better detection accuracy can be obtained [29].

B. Modeling Interleaved Attacks

We assume K distinct multi-stage attacks that are launched simultaneously in a network, and their related alerts, generated by IDS, are forwarded to the HMM database in a form of a stream of interleaved alerts. These alerts can be the result of a systematic interleaving of multiple multi-stage attacks initiated by a single attacker or can be generated randomly by different attackers. Note, for each observation length (T), we assume T alerts are processed by the HMM system. In particular, at any time, it is possible that these T alerts can be from one attack or a mix of at most K attacks. Some possible interleaved attack scenarios that can be formed systematically or randomly are described as follows:

- An attacker starts and finishes an attack (Attack 1) in the middle of another ongoing attack (Attack 2).
- Multiple attacks start and finish at different times in the presence of one or multiple ongoing attacks.
- Stages of one attack can be embedded at different times across another ongoing attack(s).
- Stages of multiple attacks can be embedded at different times of an ongoing attack(s).
- Systematic interleaving among multiple multi-stage attacks based on interleaving groups of alerts.

Existing publicly available datasets, that have multi-stage attacks, do not consider these complex attack scenarios. The DARPA2000 alerts dataset, for instance, contains two distributed denial-of-service (DDoS) multi-stage attacks that happened at different times where the attacker

uses multiple distributed compromised hosts to launch DoS attacks on a specific target [37]. To address the challenge of generating the aforementioned interleaved attack scenarios, we generate interleaved alerts by altering timestamps and IP addresses of the DARPA2000 dataset.

In order to detect the aforementioned attack scenarios, we propose two architectures based on the generic architecture shown in Fig. 1. The design of the first architecture is based on modifying HMM model parameters to deal with the interleaved alerts. Since the same alert stream is processed by all the HMM templates in the database, Architecture I suffers from high false negatives when multi-stage attacks are highly interleaved, as discussed later in the paper. Therefore, we propose a second architecture, Architecture II, to improve the detection capability by separating alerts from different attacks prior to routing alerts to HMM sub-system.

III. PROPOSED ARCHITECTURES

A. Proposed Architecture I

In order to deal with interleaved traffic alerts from different attacks, we modify HMM of the generic architecture in Fig. 1 to accommodate observations from different attacks. We assume K HMM templates are trained for K distinct multi-stage attacks. The stream of alerts generated by the IDS contains alerts that belong to one or more concurrent attacks. That is, for each observation length T, there are T observations $(o_1, o_2, \ldots, o_t, \ldots, o_T)$ processed by the HMM detection system, as shown in Fig. 2. Arrival of these alerts represents the interleaved attacks mentioned in Section II-B. The HMM_k template is trained for Attack k, therefore, out of T observations, HMM_k is expected to distinguish and process only those observations that belong to its attack, for which this HMM has been designed for. Note, among T observations, there are L_k observations (i.e., $\{o_{1_k}, o_{2_k}, \dots, o_{L_k}\}$) belong to Attack k, and the remaining $T - L_k$ observations are considered by HMM_k as unrelated (interfering) alerts. We introduce a common state that encompasses all the unrelated alerts in HMM_k . In this paper, for HMM structure, we focus on the alerts only, that is, no packets belonging to normal traffic are processed. Consequently, no normal state is considered in each HMM template. Therefore, the most likely state that can be inferred by observing $T-L_k$ unrelated observations using HMM_k is the State 1. In other words, the occurrence of these interfering observations leads to the lowest security state (State 1) in the HMM_k . To deal with these unrelated observations in parameterizing HMM_k , we introduce a new symbol, $\{o_t \notin V_k\}$, that represents all unrelated observations for Attack k. This requires modifying HMM parameters, (i. e., matrices A_k and B_k of (1)). This can be obtained by considering an observation o_t , such that $\{o_t \notin V_k\}$. Accordingly, we add an extra column in the emission probability matrix, B_k , to account for this new symbol, as follows:

$$B_k = \begin{bmatrix} b_{11} & b_{12} & \cdots & b_{1M_k} & \epsilon_1 \\ b_{21} & b_{22} & \cdots & b_{2M_k} & 0 \\ \vdots & \vdots & \ddots & \vdots & \vdots \\ b_{N_k 1} & b_{N_k 2} & \cdots & b_{N_k M_k} & 0 \end{bmatrix}$$

Note, transition to State 1, in the presence of unrelated observation o_t , occurs with probability ϵ_1 which has a very small value (such as $< 1 \times 10^{-6}$) chosen such that $\sum_{j=1}^M b_{1j} = 1$. Accordingly, almost no change is made to the other observation probabilities in the first row of the emission probability matrix. In addition, setting the probability to zero in the rest of the last column increases the probability that observing $\{o_t \notin V_k\}$ leads to State 1. A second modification is needed for the transition probability matrix (A_k) to ensure that whenever HMM_k observes the $T-L_k$ alerts from attacks other than Attack k, transition to State 1 occurs. This can be done by introducing transition probability (ϵ_2) in the first column of the A_k matrix. Although our initial assumption is a left-right model, in this architecture, instead of adding a new state to the model we let all other states return only to State 1 whenever alerts from unrelated attacks occur. An important advantage of modeling unrelated alerts in this way is that it simplifies the training of each HMM. Subsequently, by introducing ϵ_2 , matrix A_k becomes as follows:

$$A_{k} = \begin{bmatrix} a_{11} & a_{12} & \cdots & a_{1N_{k}} \\ \epsilon_{2} & a_{22} & \cdots & a_{2N_{k}} \\ \vdots & \vdots & \ddots & \vdots \\ \epsilon_{2} & 0 & \cdots & a_{N_{k}N_{k}} \end{bmatrix}$$

Based on this modification and training of the HMM template (λ_k) , the evaluation module determines whether Attack k is active or not, as shown in Fig. 2, according to the criteria $Pr(O|\lambda_k) \geq thr$. Note, thr is a threshold used to avoid unnecessary computations of the Viterbi algorithm module in case the attack is not active. The thr value can be chosen in the range of 0 to 0.5. However, with the larger the value of thr, HMM template (λ_k) estimates only the states of the high probability sequences. In this paper, we take a conservative approach in choosing thr = 0. The evaluation probability can be computed using the forward algorithm [33]. In case Attack k is active, then $three_k$ runs the Viterbi algorithm to decode the most probable

hidden states that correspond to the given observation sequence $O = \{o_1, o_2, \dots, o_t, \dots, o_T\}$, as follows:

$$x_t = \max_{1 \le i \le N_k} \gamma_t(i)$$

$$\gamma_t(i) = Pr(x_t = s_i | O, \lambda_k)$$

$$t = 1, \dots, T$$
(2)

where $\gamma_t(i)$ represents the probability of being in state s_i at time t based on the observation sequence. In Architecture I, each HMM template in Fig. 2 uses the Viterbi algorithm to find the best state sequence, $X = \{x_1, \dots, x_t, \dots, x_T\}$. For a given observation sequence, Viterbi algorithm finds the highest probability along a single path for every o_t ($t \leq T$) and o_t its corresponding state s_i such that:

$$\delta_t(i) = \underset{s_1, \dots, s_{t-1}}{\operatorname{argmax}} Pr(s_1, \dots, s_t, o_1, \dots, o_t | \lambda_k)$$
(3)

Using induction the algorithm determines the rest of the state sequence, as follows:

$$\delta_{t+1}(j) = \underset{1 \le i \le N_k}{\operatorname{argmax}} \{ \delta_t(i) a_{ij}(k) \} . b_i(o_{t+1}(k))$$
(4)

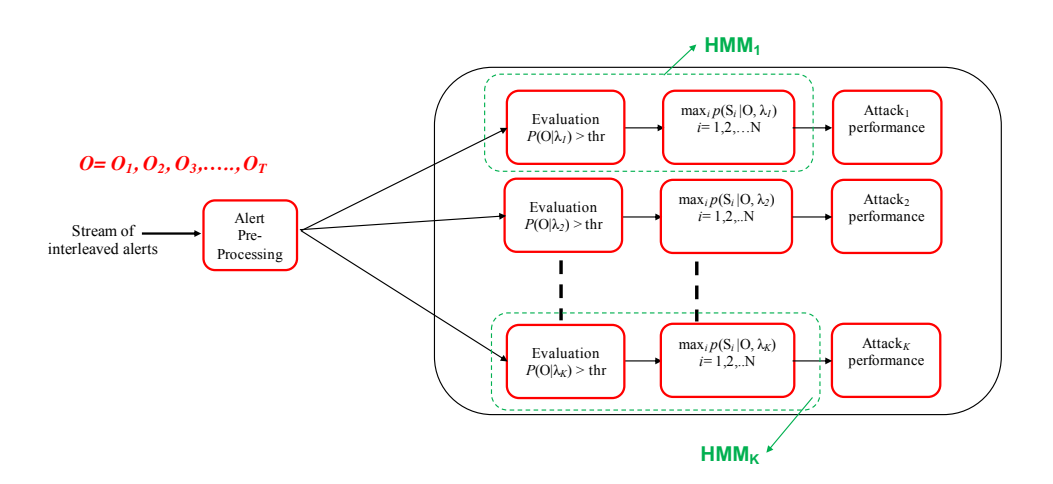


Fig. 2: Architecture I

This computation for the same given sequence is repeated by all other HMM templates in the Architecture I (Fig. 2). Table I shows the overall processing of alerts based on Architecture I. The limitation with Architecture I is that there is a high probability of high false negatives, especially when the attacks are highly interleaved. This is because each HMM template will most likely process an observation sequence that contains interfering observations belong to

other attacks. More details about detection performance of Architecture I is given in Section IV. To overcome this limitation, we propose another variation of the generic architecture of Fig. 1. The new architecture, termed as Architecture II, is depicted in Fig. 3 and is discussed below.

TABLE I: Detection process for Architecture I

```
Input: interleaved alerts: O = \{o_1, o_2, \dots, o_t, \dots, o_T\},\
      \pi_k: \lambda_k, k = 1, 2, ..., K,
      Output: X = \{x_1, x_2, \dots, x_T\}
1
      While (O is not empty)
         for k = 1 : K
2
3
          if (Pr(O|\lambda_k > thr)
4
           for t = 1:T
5
            Compute \gamma_t(i), i = 1, 2, ..., N_k from equation (2)
            x_t = \max_{1 \le i \le N_k} \gamma_t(i)
6
7
            endfor
8
           endif
9
         endfor
10
      endWhile
```

B. Proposed Architecture II

Again, we consider K interleaved multi-stage attacks that can be simultaneously launched in the network. The IDS system, based on SNORT, generates alerts from these attacks. Every alert is generated with a set of features, which includes alert ID, source/destination IP address, source/destination port number, and timestamp. In Architecture II, we use these features to improve detection efficiency of HMM templates. In particular, unrelated observations that do not belong to the k^{th} attack are separated and passed to their respective HMMs. Note, the major design philosophy behind Architecture II is to use aforementioned features to preprocess the online network traffic stream and demultiplex it into multiple substreams, as shown in Fig. 3. We refer to this preprocessing step as a demultiplexing step. It is an important step as it helps in eliminating the number of interfering observations from other attacks that are not detectable by a particular HMM.

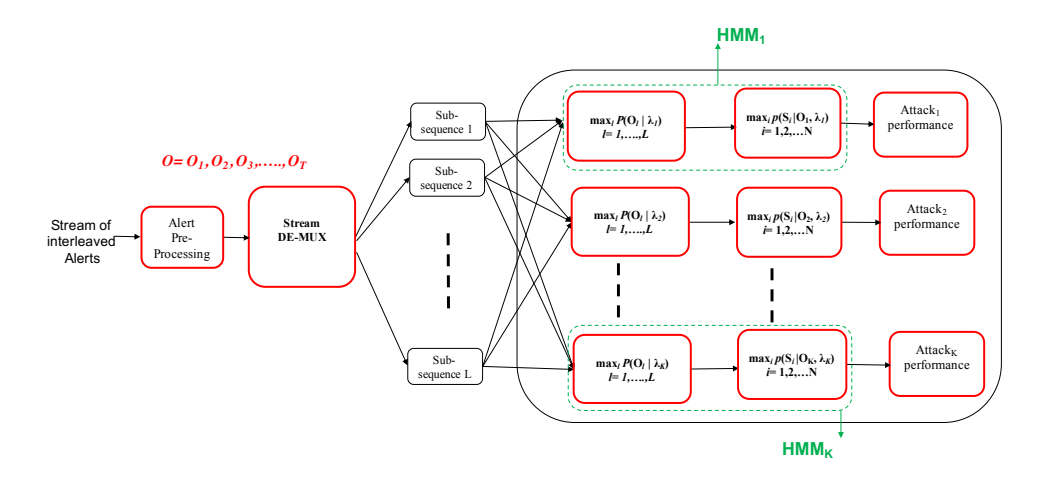


Fig. 3: Architecture II

Note, alerts triggered by the same attack scenario are correlated based on some features, (e.g., the source and destination IP addresses). We define alert (o_i) as a 7-tuple features (timestamp, ID, srcIP, srcPort, desIP, desPort, priority) according to the IDMEF [38], [39]. We refer to this tuple as a feature set $F = \{f_1, f_2, f_3, f_4, f_5, f_6, f_7\}$. The timestamp represents date and time of an alert generated by the IDS. ID is the identification of the alert, srcIP and srcPort indicate the source IP address and source port number, respectively. Also, desIP and desPort represent the destination IP address and port number, respectively, and priority indicates the alert's rank [10].

A subset, S, from the feature set F ($S \subset F$) can be used for demultiplexing operation. The simplest way in which we can demultiplex interleaved alerts is by grouping the alerts that are triggered by the same multi-stage attack into a one subsequence based on their IP addresses relationships, as illustrated in Fig. 4, i.e., $S = \{f_3, f_5\}$. Note, IP addresses of the alerts, which are triggered by the same attack scenario, are generally related. Consider that there are two alerts, o_i and o_j . The demultiplexer searches for these addresses to check if they have the same srcIP, or the same desIP. Moreover, it also checks whether destIP of the previous alert is the same as the srcIP of the next one, as in a multi-stage attack scenario, the destination node of an earlier alert is the source node of the next alert. Based on the IP address search, the demultiplexer either inserts o_i and o_j in the same subsequence or in different ones.

The demultiplexer performs stream demultiplexing function into L substreams $(1 \le L \le K)$. The demultiplexing process is based on one or more aforementioned distinguishing feature(s) of the incoming alerts. Therefore, from the incoming stream of alerts, $O = \{o_1, o_2, \dots, o_t, \dots, o_T\}$,

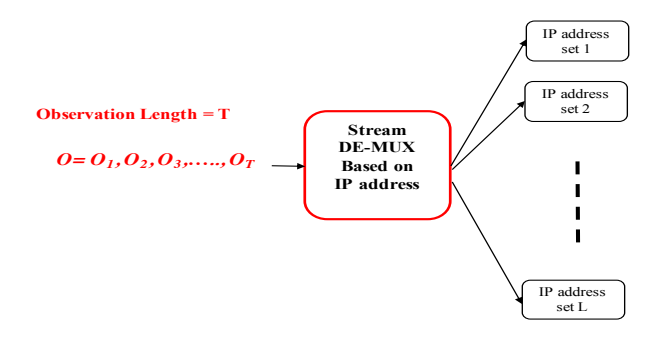


Fig. 4: Alert sequence demultiplexed into multiple subsequences based on IP addresses only

the demultiplexer generates L substreams each of which belongs to a distinct multi-stage attack. These substreams are a subset of O, which are represented as, $O_1 = \{o_{1_1}, o_{2_1}, \dots, o_{T_1}\}$, $O_k = \{o_{1_k}, o_{2_k}, \dots, o_{T_k}\}$, and so on till $O_L = \{o_{1_L}, o_{2_L}, \dots, o_{T_L}\}$, where $L \leq K$ and $T_k \leq T$. Note, the larger the feature subset we consider in stream demultiplexing, the more distinct substreams we obtain and, in turn, the more processing is entailed. Note, within an observation sequence, alerts can belong to L attacks where $1 \leq L \leq K$.

The demultiplexer module does not distinguish among types of attacks, therefore, it cannot route a substream to its corresponding HMM template. To address this issue in Architecture II, each HMM can have L instances, each of which can process one single substream. Thus, all the L generated substreams pass through each HMM to find which subsequence matches a certain HMM. The computation by each instance is performed based on the posterior probability given in (5).

$$O_k^* = \max_{1 \le l \le L} Pr(O_l | \lambda_l), \quad L \le K$$
(5)

Note, this probability computation is performed $L \times K$ times. The next stage of the HMM process is to estimate state probabilities for its corresponding subsequence, O_k^* , found from (5) using the Viterbi decoding algorithm, as follows:

$$x_t = \max_{1 \le i \le N_k} \gamma_t(i)$$

$$\gamma_t(i) = Pr(x_t = s_i | O_k, \lambda_k)$$

$$t = 1, \dots, T_k$$
(6)

Unlike Architecture I, the first stage of every HMM in Architecture II has a maximum of K instances of the forward algorithm and one instance of the Viterbi algorithm. In addition, the

TABLE II: Detection process for Architecture II

```
Input: interleaved alerts: O = \{o_1, o_2, \dots, o_t, \dots, o_T\},\
      \pi_k: \lambda_k, k = 1, 2, \dots, K,
      Output: X = \{x_1, x_2, \dots, x_T\}
1
      While (O is not empty)
        Demultiplex sequence O into L subsequences, O_1, O_2, \ldots, O_L
2
3
          for k = 1 : K
4
            for l = 1 : L
5
             Compute (Pr(O_l|\lambda_k)
6
            endfor(l)
            Find O_k^* = \max_{1 \le l \le L} Pr(O_l | \lambda_k)
7
8
             for t = 1 : T_k, T_k is the length of sequence O_k^*
9
               Compute \gamma_t(i) = Pr(x_t = s_i | O_k^*, \lambda_k), from equation (6)
10
              x_t = \max_{1 \le i \le N_k} \gamma_t(i)
11
             endfor(t)
12
          endfor(k)
13
      endWhile
```

HMM in Architecture II deals with subsequences of length T_k , where $T_k \leq T$. Table II shows the overall processing of alerts based on Architecture II.

C. Complexity Comparison between Proposed Architectures

Note, in Architectures I and II in Figs. 2 and 3, the main modules that contribute to the computational complexity are the alert preprocessing module for assigning alert severity, the stream demultiplexing module, and the HMM parallel branch modules. The first preprocessing module is the same for both architectures; however, the demultiplexing module exists only in Architecture II, which requires a demultiplexing of all T alerts based on a subset S of alert features considered in the demultiplexing operation. The larger the S and S sets are, the more complex computation is required by this module. In other words, Architecture II has S and S additional complexity requirement as compared with Architecture I as a result of the demultiplexing operation.

Next, we consider the HMM database component of the architectures. Note, two algorithms

are needed to be executed in each branch of the HMM database; the Forward (FW) algorithm to compute posterior probability for the evaluation purpose and the Viterbi algorithm to estimate the best state sequence. In Architecture I, every incoming sequence of T alerts is processed by all K branches. In other words, K computations of FW algorithm plus K computations of Viterbi algorithm are performed. On the other hand, in Architecture II, each HMM module deals, on the average, with a shorter sequence length compared to the case in Architecture I. In the first module of each branch, FW algorithm is required to be executed L times, and in the second module of the branch, the Viterbi algorithm is executed once. Therefore, in Architecture II, $L \times K$ computations of FW algorithm plus L computations of the Viterbi algorithm are performed. It is important to note that although Architecture II seems to perform more number of computations in HMM database, the length of sequences processed by both FW and the Viterbi algorithms is, on the average, shorter than the sequences in Architecture I. The primary shortcoming of Architecture II is the computation overhead needed for the demultiplexing operation. This overhead can be high especially for the case of a large value of T and a large number of features.

IV. EVALUATION AND PERFORMANCE MEASURES

In this section, we discuss our experimental results based on the DARPA2000 dataset [37], which contains two DDoS multi-stage attacks labeled as LLDDOS 1.0 and LLDDOS 2.0.2. Both of these attacks have five stages, that can be summarized as IP sweeping, Sadmind probing, Sadmind exploit, DDoS software installation and Launching. In our experiment, DARPA2000 raw network packets were processed by SNORT intrusion detection system [34] to generate alerts. The total number of alerts results from this process is 3500 and 2000, for LLDDOS 1.0 and LLDDOS 2.0.2 attacks, respectively. These alerts are clustered into 12 distinct symbols. Therefore, $M_k = 12, k = 1, 2$, as mentioned in Section II-A. The preprocessing module assigns a severity level to these alerts based on their relation to the stages of multi-stage attacks. In case there are more than one alert which lead to a state, the higher the severity level is given to the alert which indicates that the attack is progressing. Accordingly, Tables III and IV show alert severity, alert type and states of both attacks [26].

The training of the two HMMs is conducted based on a five state model ($N_k = 5, k = 1, 2$), which corresponds to five stages in each attack. The state diagrams of HMM1 for Attack 1 and HMM2 for Attack 2 are shown in Fig. 5. The parameterization of each HMM is given in Appendix A. The training of HMMs in terms of computation of observations and states

Alert Severity	Alert Type ICMP PING					
1						
2	ICMP Echo Reply					
3	ICMP PING BSDtype					
4	ICMP PING Unix					
5	RPC portmap sadmind request UDP attempt					
6	ICMP Destination Unreachable Port Unreachable RPC sadmind UDP PING RPC sadmind query with root credentials attempt UDP					
7						
8						
9	RPC sadmind UDP NETMGT CLIENT overflow attempt					
10	SERVICES rsh root	4				
11	TELNET login					
12	SNMP AgentX/tcp request	5				
	and flood DDoS attempt					

Alert Severity	Alert Type					
1	RPC portmap sadmind request UDP					
2	RPC portmap Solaris sadmind port query udp request					
3	RPC portmap Solaries sadmind port query					
4	udp portmapper sadmind port query attempt					
5	RPC sadmind query with root credentials attempt UDP					
6	RPC sadmind UDP					
7	sadmind UDP NETMGT CLIENT overflow attempt					
8	RPC portmap Solaries sadmind port query - Diff. IP					
9	RPC sadmind query with root credentials attempt UDP - Diff. ${\it IP}$	3				
10	RPC sadmind UDP - Diff. IP	4				
11	sadmind UDP NETMGT CLIENT overflow attempt - Diff. IP	4				
12	ICMP Destination Unreachable Port Unreachable	5				
	and flood DDoS attempt					

TABLE III: Correspondence between Alert type, Alert Severity and States in DARPA LLDDOS 1.0

TABLE IV: Correspondence between Alert type, Alert Severity and States in DARPA LLDDOS 2.0.2

probabilities are based on the machine learning toolbox in MATLAB [40]. For the purpose of training, we use 30% of the dataset, while the rest of the dataset was used for testing. In this evaluation, parameters ϵ_1 and ϵ_2 of models λ_1 and λ_2 of Architecture I are chosen as $\epsilon_1 = 10^{-6}$ and $\epsilon_2 = 10^{-3}$.

For the completeness of our evaluation, we present the detection performance of the two multistage attacks using their respective HMMs when these attacks occur one at a time. Subsequently, several scenarios of the two simultaneous attacks are generated with a varying degree of interleaving to test the performance of the proposed architectures. For some cases, we compare the three architectures of Figs. 1, 2, and 3. The reason for using the generic architecture of Fig. 1 for the comparison is that, no evaluation has been done in the literature for multiple multistage attacks. For all the results, the x-axis shows the running count of alerts as they are generated by SNORT. For the purpose of evaluation, we propose three performance metrics, in addition to the widely used state probability metric [26]. The proposed metrics are: (1) attack risk probability which provides an insight about the speed of attacks and can help in prioritizing response actions, (2) detection error rate performance, which measures how much error is generated by an architecture in estimating states, and (3) the number of correctly detected stages. The justification of these performance metrics is given in the following subsections.

A. Detection of Individual DARPA2000 Attacks

In this subsection, we first consider the alerts generated by SNORT when only LLDDOS 1.0 dataset is used. We pass these alerts to the alerts preprocessing module and then to HMM1

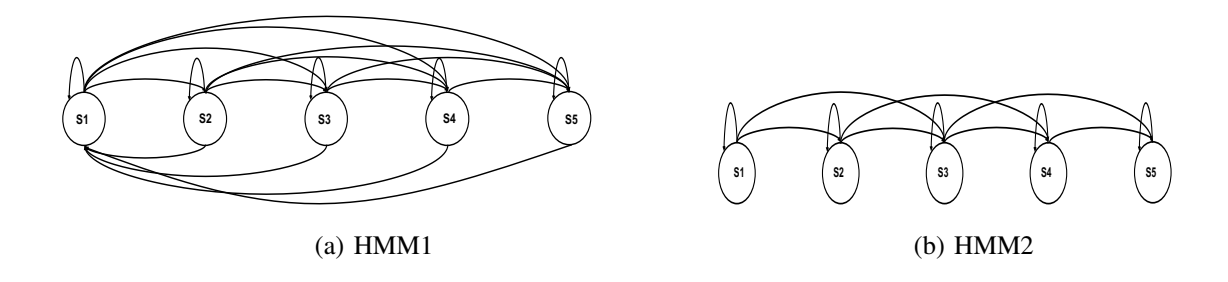


Fig. 5: State Diagrams for HMM1 and HMM2

which is trained to detect the first DDoS attack (Attack 1). The same is done for LLDDOS 2.0.2 dataset to detect the second DDoS attack (Attack 2). The state probability results of each attack is shown in Fig. 6. It can be noted that the five stages of each attack are detected by each HMM. It can also be noted that Attack 2 is relatively faster than Attack 1, as few alerts are needed by Attack 2 to reach the last stage of HMM2 indicating the launching of the DDoS attack on the target. In Fig. 6 we show the estimated state corresponding to only the first 500 alerts out of all the SNORT alerts as the remaining alerts are almost all the same and lead to the compromise state (State 5). The observation length for this case is taken as T = 100.

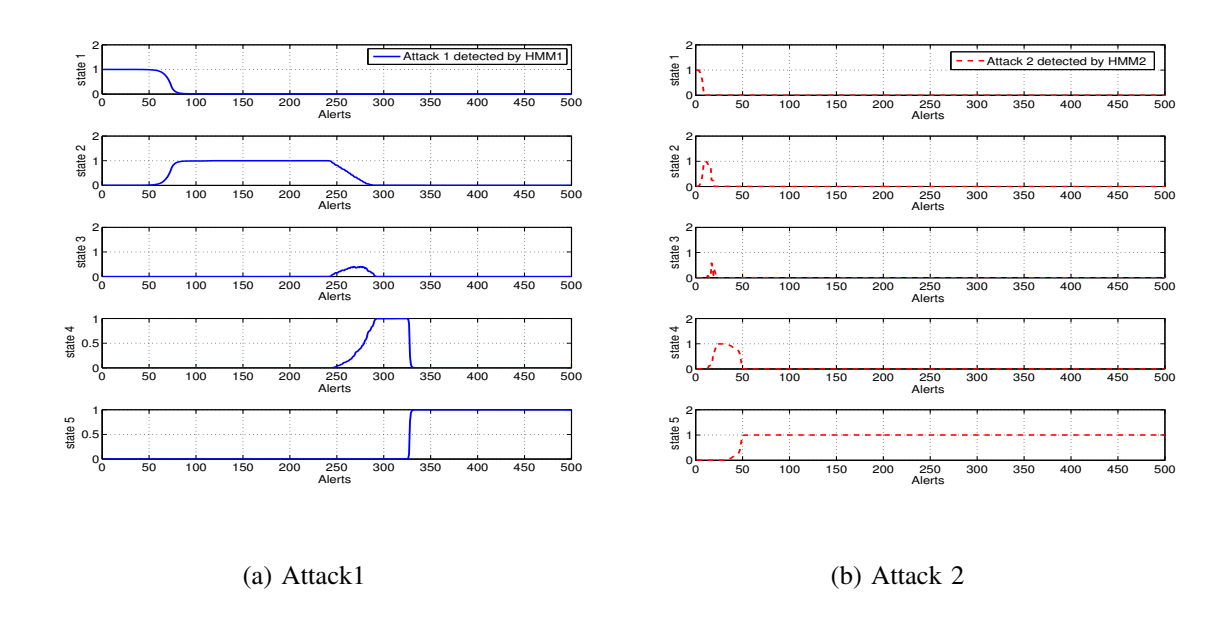


Fig. 6: State probability of HMM1 and HMM 2 for individual DARPA attacks

B. Generating Alerts Interleaving Scenarios

Based on the two multi-stage attacks in the DARPA2000 dataset, we altered the timestamp of some of alerts in both attacks so that we can generate a single sequence of alerts that is composed of a mix of the two attacks without altering the temporal order of the original alerts. In addition, the IP addresses of the hosts attacked by Attack 2 (LLDDOS 2.0.2) are also changed. The reason for this modification is to simulate two simultaneous attacks intruding a network. Fig. 7 shows several scenarios of interleaved alerts for two simultaneous DDoS attacks. Note, the degree of interleaving increases from Scenario 1 to 4 indicating more sophistication of actions and complexity of attacks. Since Attack 2 takes shorter time to compromise the target and launch DDoS, we manipulate timestamps of Attack 2 so that it spreads across different times of Attack 1. The y-axis in Fig. 7 represents the alert severity based on the preprocessing module as depicted in Tables III and IV. Based on these scenarios the performance results of the proposed architectures are given in the following subsections.

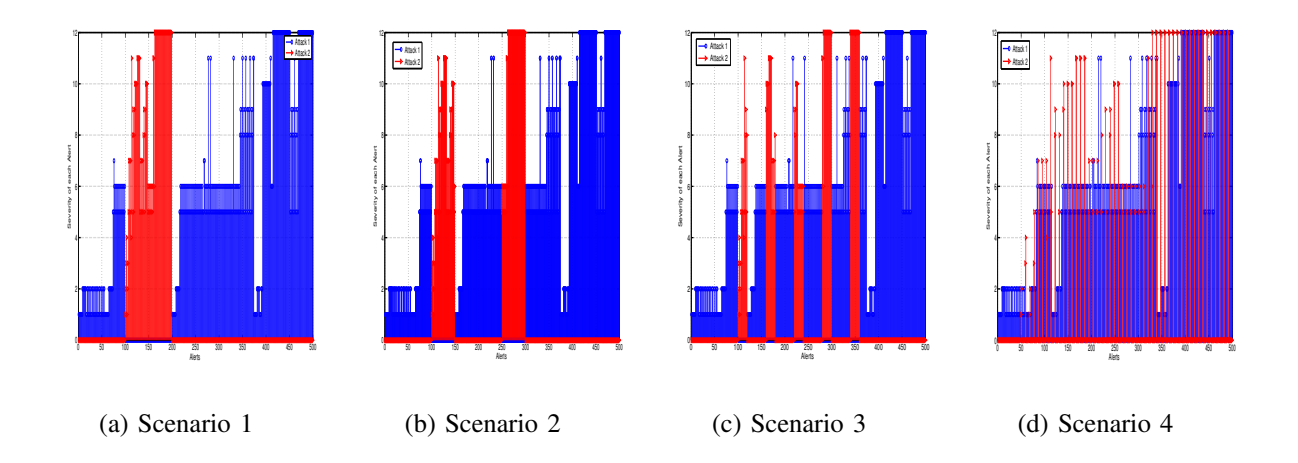


Fig. 7: Interleaved alerts scenarios from LLDDOS 1.0 and LLDDOS 2.0.2 attacks

C. Probability of State Estimation and the Effect of Interleaving

In this subsection, we present the state probability, $\gamma_t(i)$, from (2) and (6) for i = 1, ..., 5 with two observation lengths, T = 10 and T = 500. For T = 500, it can be seen from Figs. 8a and 8b that Architecture I can estimate¹ the states of both attacks with a high probability, especially

¹Note: The terms detecting a state and estimating a state are used interchangeably in this paper

for States 1, 2, 4, and 5. However, as the degree of interleaving increases from Scenario 1 to Scenario 4, Architecture I fails to detect many states. For example, for Scenario 3, States 3 and 4 of Attack 2 are not detected, as depicted in Fig. 8c. For Scenario 4, Architecture I performs very poorly as it fails to detect all the states of both attacks, as depicted in Fig. 8d. For T=10, Architecture I shows a small improvement in detecting States 3 and 4 for Scenarios 1 and 3, respectively, as can be seen from Fig. 8 and Fig. 10. The reason for this poor performance of Architecture I, is that as the degree of interleaving between alerts increases, the more interfering alerts can exist within a given sequence, causing the Viterbi algorithm to incorrectly determine the state probability of the non-interfering alerts.

Architecture II, on the other hand, performs better as compared to Architecture I in terms of estimating correct states of all incoming alerts for both T=10 and T=500. This performance improvement even for a higher degrees of interleaving can be observed from Figs. 8c, 8d, 9c, 9d, 10c, 10d, 11c, and 11d. The reason behind this performance improvement for Architecture II is the presence of the demultiplexing module that helps each HMM to process only relevant attack alerts. Note, for both architectures the state probability for State 3 of Attack 1 is very low for both values of T. The reason is there are not enough alerts produced by SNORT for this stage.

We observe discontinuity in the state probability plot of Architecture I in Figs. 8 and 10, which is due to the fact that both HMMs return to State 1 whenever there exist interfering alerts from other attacks. However, in Architecture II, as the alerts from different attacks are demultiplexed prior to their processing by HMMs, the states of HMMs are not interrupted. Fig. 12 shows the importance of considering ϵ_2 in designing HMM used by Architecture I. In this experiment, we choose $\epsilon_2 = 0.001$, which is a small value that does not significantly affect the transition probability matrices, A_1 and A_2 , obtained from training. Note, $\epsilon_2 = 0$ represents the case of generic architecture, for which returning to State 1 is not allowed when HMM1 receives alerts belong to Attack 2 or when HMM2 receives alerts belong to Attack 1. Setting $\epsilon_2 = 0$ reduces the accuracy of state detection for the two attacks, as can be seen in Fig. 12. For example, for interleaving Scenario 2, Fig. 12a provides no estimate for state probability of States 2 and 4 for the first 200 alerts when $\epsilon_2 = 0$, as compared to Fig. 12b when $\epsilon_2 = 0.001$. Similar observation can be made by comparing Figs. 12c and 12d for the first 350 alerts of State 2.

In summery, Figs. 8, 9, 10, and 11 show that there is no significant change in the state detection performance of each architecture as the observation length changes from 10 to 500 alerts.

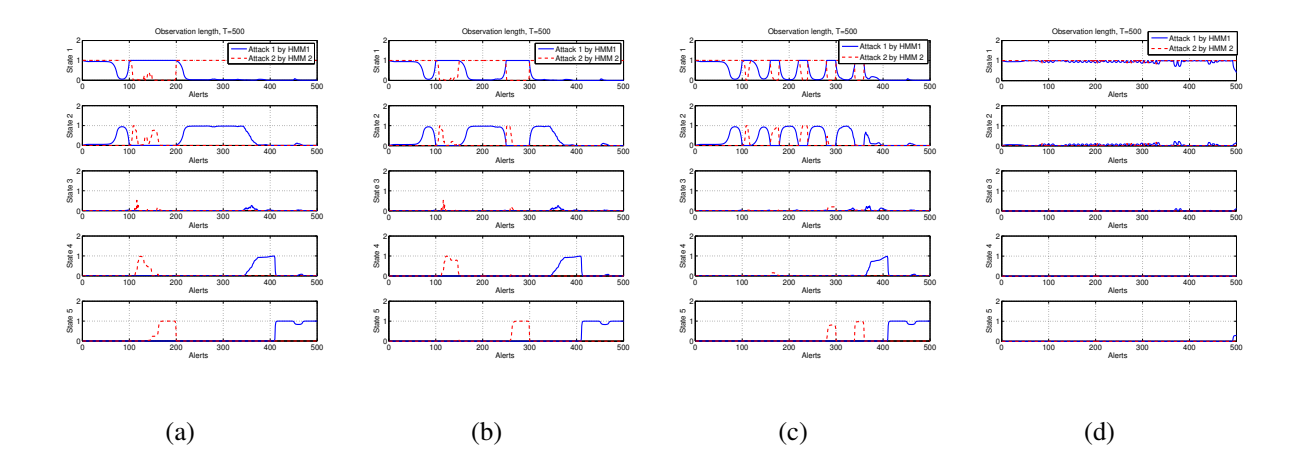


Fig. 8: State probability of Attacks 1 and 2 detected by HMM1 and HMM2 based on Architecture I, T=500

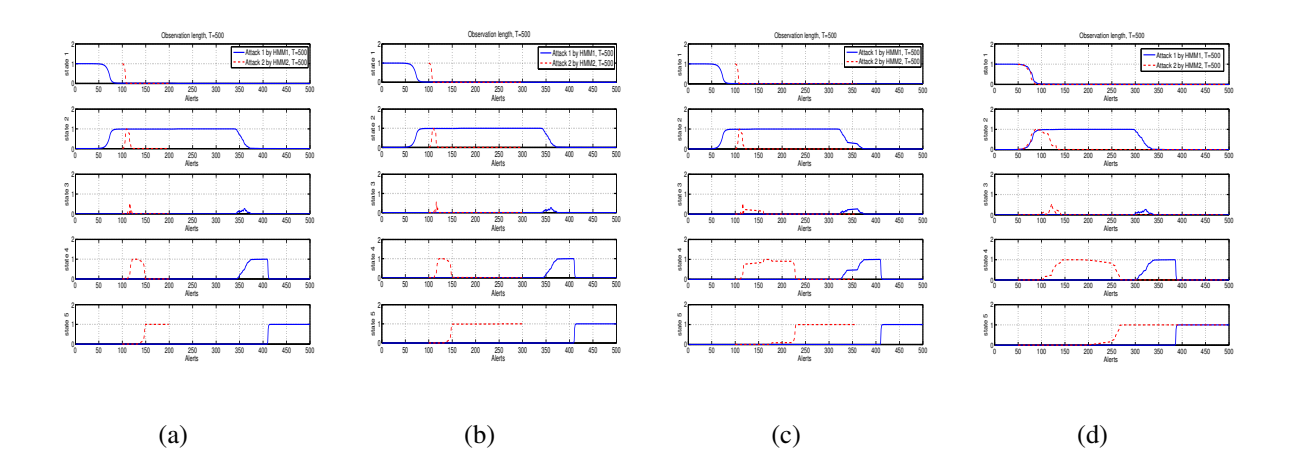


Fig. 9: State probability of Attacks 1 and 2 detected by HMM1 and HMM2 based on Architecture II, T=500

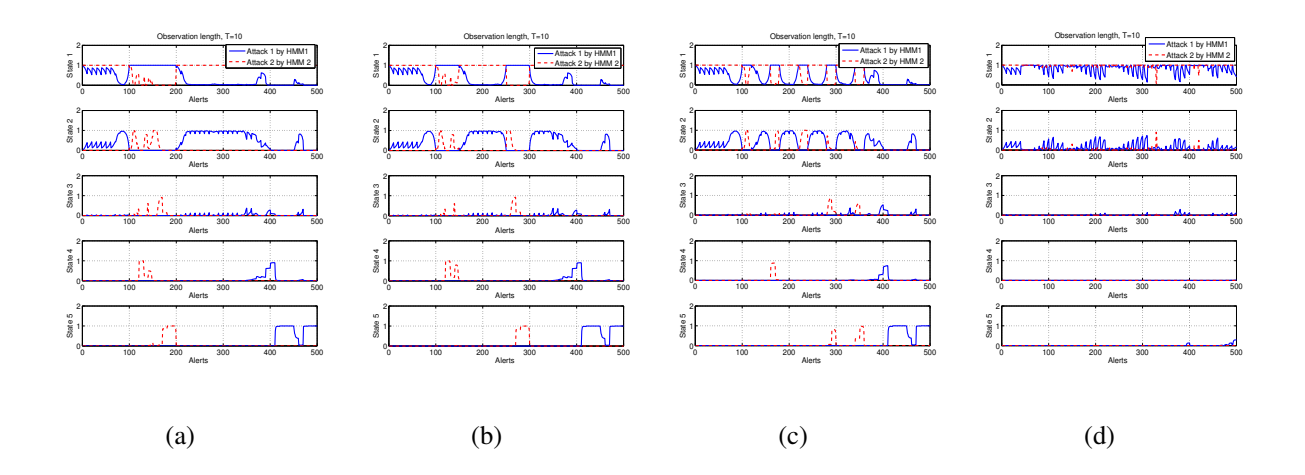


Fig. 10: State probability of Attacks 1 and 2 detected by HMM1 and HMM2 based on Architecture I, T=10

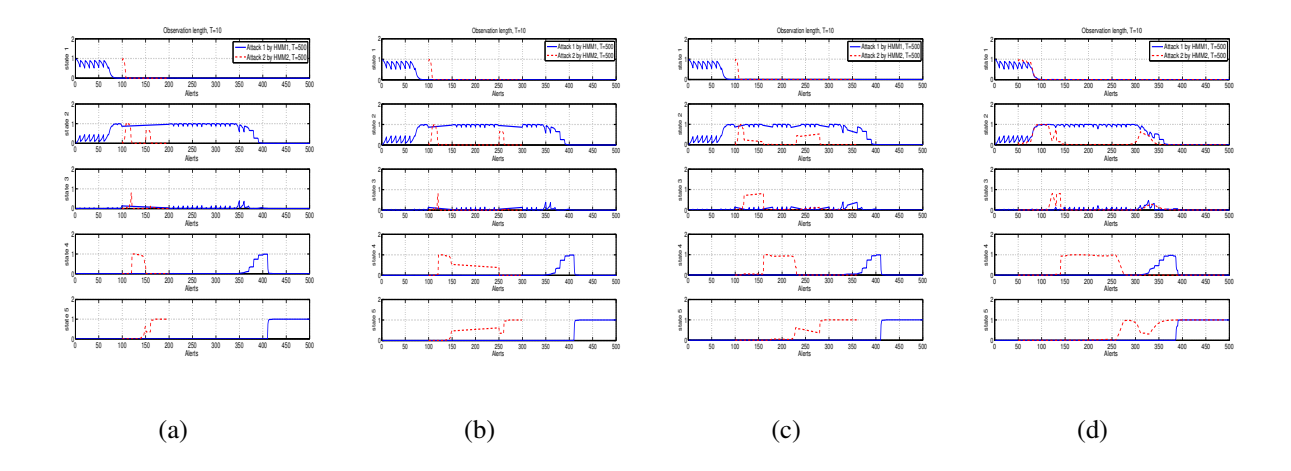


Fig. 11: State probability of Attacks 1 and 2 detected by HMM1 and HMM2 based on Architecture II, T=10

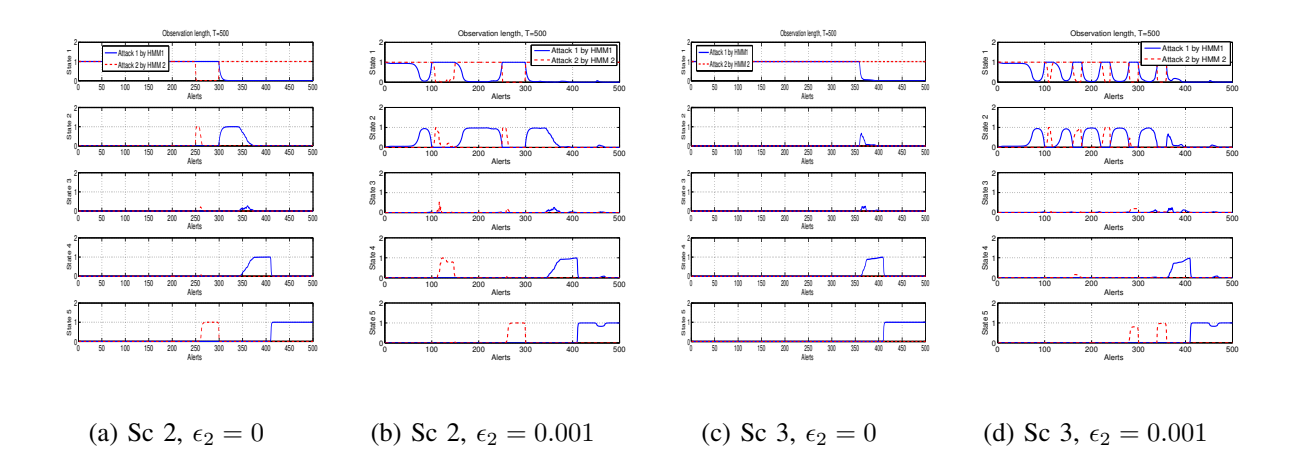


Fig. 12: Effect of ϵ_2 on state probability based on Architecture I

Moreover, Architecture II is more robust in terms of having better state probability estimation metric at a higher degree of interleaving as compared to Architecture I.

D. Attack Risk Probability

We define the first proposed performance metric as the attack risk probability, which is the probability of how far an attack is from compromising the target, i. e., reaching the final state. The calculation of this attack probability depends on the estimated state probability ($\gamma_t(i)$) averaged over the total number of states. Its value gets updated at every observation length in a non-

decreasing manner, as shown below in (7):

$$Pr_{attack_k}(t) = \frac{\sum_{i=1}^{N_k} \gamma_t(i) s_i}{N_k}$$

$$t = 1, \dots, T \ i = 1, \dots, N_k, \ k = 1, \dots, 2$$
(7)

This performance measure can help in tracking the progress of each attack, especially when there are multiple organized attacks. It can be noted that, the rate at which the attack risk probability changes with respect to alerts gives an indication of how fast or slow an attack is progressing. Consequently, this measure can help in prioritizing response actions for each ongoing attack.

Figs. 13 and 14 show the attack risk probability for both DARPA multi-stage attacks using Architecture I and II for different interleaving scenarios and for the two observation lengths, T=10 and T=500. The results shown are for Scenarios 3 and 4, as they are relatively more complex to detect. Fig. 14 shows that Architecture II can track the progress of Attacks 1 and 2 for both interleaving scenarios accurately based on the knowledge of the generated input alerts shown in Figs. 7c and 7d. Note, there is no significant difference between the case of T=10, and T=500. Also note, after 100 alerts, Attack 2 progresses relatively fast, and reaches the compromise state well before Attack 1. However, on the other hand, Architecture I underestimates the progress of Attacks 1 and 2, as shown in Figs. 13c and 13d. This is because Architecture I fails to detect some of the states for Scenarios 3 and 4, as illustrated in the previous subsection. Fig. 13c shows that both attacks progress at a slow pace. However, this is not true as depicted in Fig. 14c where Architecture II shows both attacks progress fast at different paces. For instance, Attack 2 reaches 80% after 100 alerts, while Attack 1 reaches 80% after 300 alerts. Moreover, Fig. 13d shows that Attack 1 progresses faster than Attack 2, which is also not true, as depicted in Fig. 14d that indicates Attack 2 is faster than Attack 1. This inaccurate detection of these attacks can adversely affect response decisions, especially, when a priority-based response mechanism is employed [1].

E. Error Rate Performance

The next performance measure we propose is the error rate (ER), which is the ratio of the number of errors due to the inconsistency between the type of an alert and the corresponding estimated state to the total number of incoming alerts. Formally, ER is given by the following equation:

$$ER = \frac{\text{Number of incorrect detected states of the incoming Alerts}}{\text{Total number of Alerts}} \times 100$$
 (8)

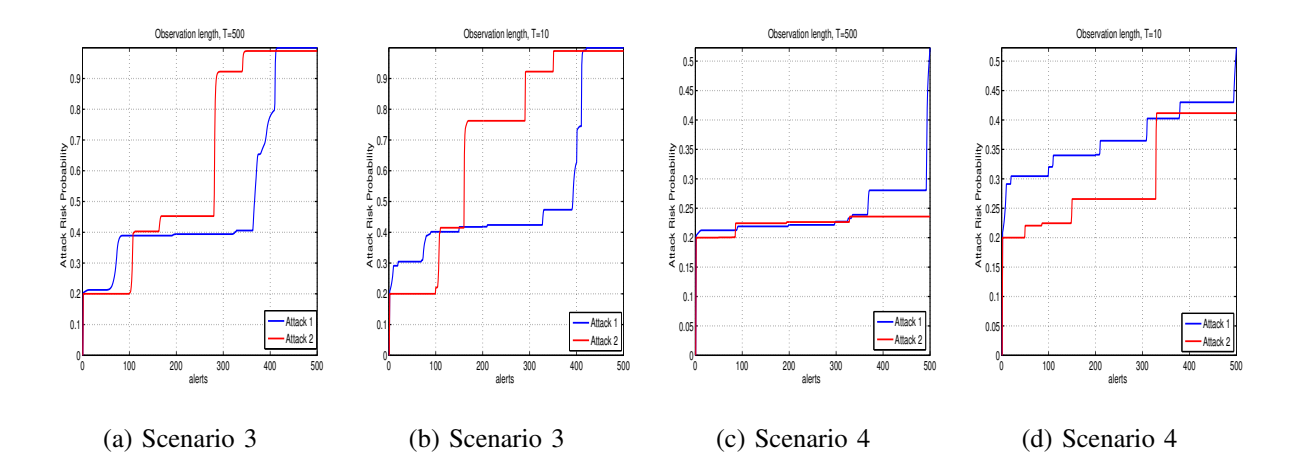


Fig. 13: Attack risk probability based on Architecture I

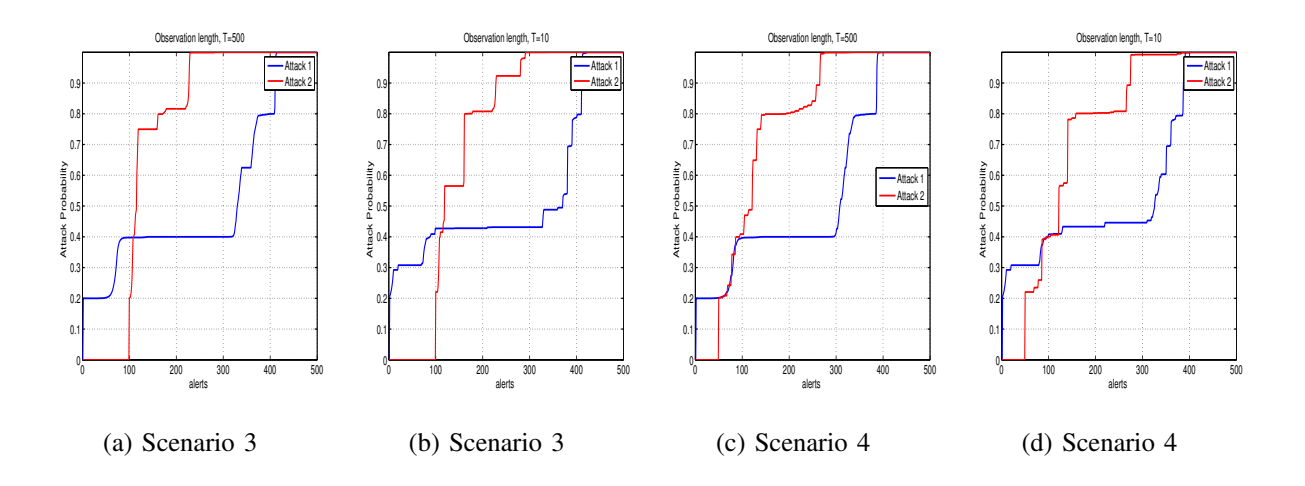


Fig. 14: Attack risk probability based on Architecture II

Note, the exact state corresponding to every incoming alert is considered based on the knowledge of the input alerts and their corresponding states, according to Tables III and IV. Note also, ER is equivalent to the false negative rate. The reasons for inconsistency between type of alerts and their detected states are: (1) the presence of interfering alerts, and (2) the state estimation error resulted from the enforcement of the left-right HMM model.

Fig. (15) shows the plot of ER for different interleaving scenarios and for several values of T. It can be seen from the figure that the proposed architectures outperform generic architecture (Fig. (1)) for interleaving Scenarios 1,2, and 3. However, for Scenario 4, both Architecture I and generic architecture have similar ER, which is higher than Architecture II. It can also be

noted that the ER for Architecture II remains almost constant with respect to T and is also the same for all scenarios. Similarly, Architecture I has almost constant ER with respect to T. However, its ER performance gets worse as the degree of interleaving increases as compared to Architecture II. For instance, for Scenario 4, ER for Architecture I is as high as 77% as compared to Architecture II which has a value of 22%.

Note, for generic architecture, the ER generally increases with T and saturates to a value. The main reason is the same as aforementioned reason (1) and the lack of capability of this architecture to distinguish between alerts from two different attacks. In addition, due to the same reason, its ER also increases from Scenario 1 through Scenario 4.

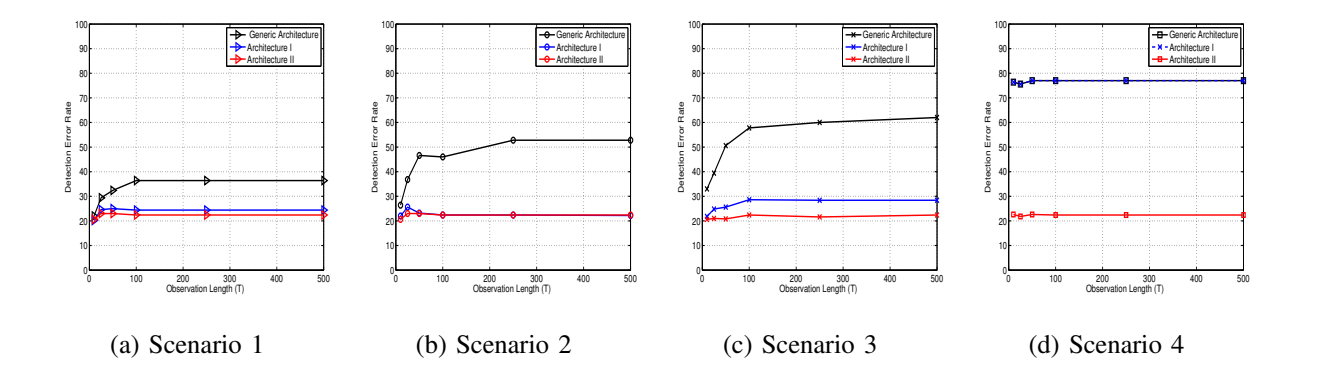


Fig. 15: State detection error rate at various interleaving scenarios

F. Number of Correctly Detected Stages per Attack

The third performance measure we propose is the number of correctly detected stages per attack, which allows us to analyze the security impact due to missing or incorrectly detecting stages in a multi-stage attack, especially from the point of view of considering response actions. We compare between architectures in terms of the number of detected stages per attack.

This measure is computed as follows. As we know the correspondence between alerts and stages (or states) of the attacks based on the knowledge of the DARPA2000 dataset, as shown in Tables III and IV, we compare the estimated states from each HMM with the exact states. Table V provides the results for three different values of T. It can be observed that Architecture II outperforms Architecture I in correctly detecting more stages for both attacks. The performance of the two architectures is the same for the interleaving Scenario 2, as both of them can detect stages 1, 2, 4, and 5 but not 3. This can also be seen in Figs. 8b, 9b, 10b, and 11b.

For Scenarios 3 and 4, Architecture II detects more stages than Architecture I. For example, all five stages of Attack 2 are detected in Scenario 3 using Architecture II for T=500, while Architecture I only detects Stages 1 and 5. Fig. 16 shows the estimated states by HMM2 for Attack 2 using Scenario 3. It can be observed that with Architecture I, Stages 3 and 4 are not detected. The advantage of Architecture II can be more apparent in Table V when the interleaving Scenario 4 is used.

Fig. 16 and Table V show the importance of this performance metric in terms of how much lead time is available to respond to ongoing attacks. For instance, Fig. 16b shows that Architecture I detects State 2 then immediately detects State 5 of Attack 2, which implies that there is no enough lead time available to respond to a progressing attack. While, on the other hand, Fig. 16c shows that Architecture II detects all states of Attack 2 in a correct sequence similar to the synthesized input states of Attack 2 shown in Fig. 16a. This performance metric establishes the importance of considering a large number of states in modeling HMM in essence that the effect of missing a few number of sates does not drastically impact the lead time while making real time response decisions to an ongoing multi-stage attack.

TABLE V: Number of Correctly Detected Stages per Attack at Various Interleaving Scenarios

Interleaving Scenario	Architecture	Attack	T = 10	T = 100	T = 500
	I	Attack 1	4	4	4
Scenario 2	1	Attack 2	5	5	5
Scenario 2	П	Attack 1	4	4	4
		Attack 2	5	5	5
	I	Attack 1	4	4	5
Scenario 3		Attack 2	4	4	3
Scenario 5		Attack 1	4	5	5
		Attack 2	5	5	5
	I	Attack 1	1	1	1
Scenario 4		Attack 2	1	1	1
Scenario 4	II	Attack 1	4	5	5
		Attack 2	5	5	5

G. Extension to a higher number of attacks

The evaluation experiments in this paper were implemented with two simultaneous interleaved attacks because of the limited available datasets of multiple attacks. However, it can be observed that our proposed architectures can work easily with more than two simultaneous attacks. In particular, Architecture II can perform well since it depends essentially on the demultiplexing

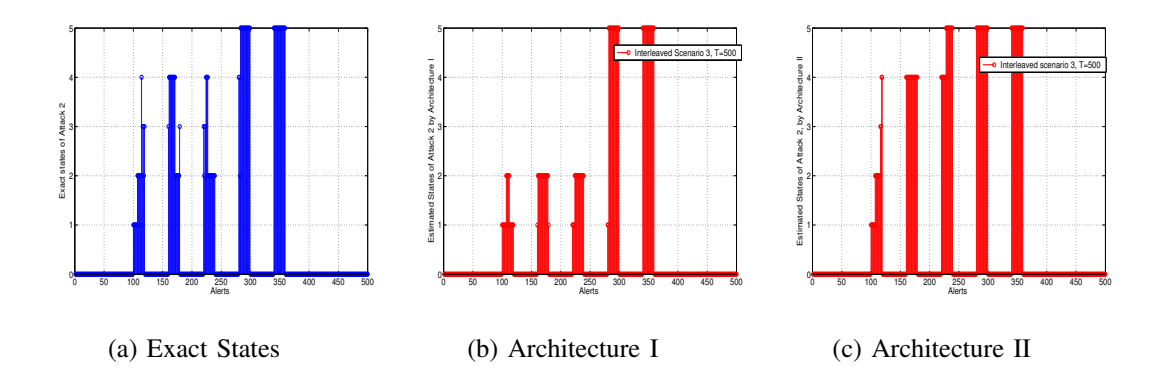


Fig. 16: Comparison between Architectures I and II in detecting stages of Attack 2 for Scenario 3

operation. With more than two attacks, we expect more computations, especially in the demultiplexing module and also in the HMM database component. Architecture I can also work well with more than two attacks, but its detection performance deteriorates significantly with a large number of attacks and a higher degree of interleaving.

V. CONCLUSION

This paper addresses the detection problem of interleaved multiple multi-stage attacks intruding a computer network. We propose two architectures based a well known machine learning technique, i. e. Hidden Markov Model, and provide their performance results and computational complexity. Both architectures can track interleaved attacks by obtaining the correct states of the system for each incoming alert. However, as the degree of interleaving among attacks increases, Architecture II, which employs a demultiplexing mechanism, exhibits better performance as compared to Architecture I. For performance assessment of these architectures, we propose three performance metrics which include (1) attack risk probability, (2) detection error rate, and (3) the number of correctly detected stages.

VI. ACKNOWLEDGMENT

This research was supported by the grants from Northrop Grumman Corporation and US National Science Foundation (NSF) Grant IIS-0964639.

APPENDIX A

HMM PARAMETERS

The two HMMs are trained using 30% of the DARPA2000 dataset, i.e. HMM1 is using LLDDOS 1.0 and HMM2 is using LLDDOS 2.0.2 for training, while the rest of the dataset was used for testing. The main parameters of HMM model in both attacks are determined from training using the BW algorithm using MATLAB, and they are as follows:

$$A_1 = \begin{bmatrix} 0.8550 & 0.1448 & 0.0001 & 0.0001 & 0.0001 \\ 0 & 0.9 & 0.0997 & 0.0001 & 0.0001 \\ 0 & 0 & 0.9880 & 0.0090 & 0.0001 \\ 0 & 0 & 0 & 0.9880 & 0.0090 \\ 0 & 0 & 0 & 0 & 1 \end{bmatrix}, \ A_2 = \begin{bmatrix} 0.9287 & 0.0712 & 0.0001 & 0 & 0 \\ 0 & 0.9141 & 0.0857 & 0.0001 & 0 \\ 0 & 0 & 0.9387 & 0.0612 & 0.0001 \\ 0 & 0 & 0.9752 & 0.0248 \\ 0 & 0 & 0 & 0.9999 & 0.0656 & 0.0970 & 0.0467 \\ 0 & 0.0844 & 0.1088 & 0.0803 & 0.0965 & 0.0593 & 0.0333 \\ 0 & 0.0955 & 0.0638 & 0.1138 & 0.1163 & 0.0201 & 0.1162 & 0.0536 & 0.1211 & 0.1127 & 0.1165 & 0.0577 & 0.0451 \\ 0 & 0.0927 & 0.0707 & 0.0771 & 0.0947 & 0.0349 & 0.1927 & 0.0115 & 0.0844 & 0.0553 & 0.0032 & 0.0207 & 0.1142 \\ 0 & 0.9922 & 0.0651 & 0.1968 & 0.0427 & 0.1096 & 0.0941 & 0.1127 & 0.0089 & 0.0886 & 0.0358 & 0.0800 & 0.0736 \\ 0 & 0.0630 & 0.0568 & 0.1421 & 0.0052 & 0.0007 & 0.1598 & 0.1049 & 0.0798 & 0.0519 & 0.1332 & 0.0955 & 0.1071 \\ 0 & 0.0459 & 0.1605 & 0.1204 & 0.1586 & 0.0158 & 0.0075 & 0.1319 & 0.1817 & 0.1053 & 0.0160 & 0.0521 & 0.0041 \\ 0 & 0.0356 & 0.0408 & 0.0978 & 0.0841 & 0.0290 & 0.1304 & 0.0411 & 0.1242 & 0.1427 & 0.0693 & 0.0357 & 0.1693 \\ 0 & 0.0356 & 0.0408 & 0.0978 & 0.0841 & 0.0290 & 0.1304 & 0.0411 & 0.1242 & 0.1427 & 0.0693 & 0.0357 & 0.1693 \\ 0 & 0.0356 & 0.0408 & 0.0978 & 0.0841 & 0.0290 & 0.1304 & 0.0411 & 0.1242 & 0.1427 & 0.0693 & 0.0357 & 0.1693 \\ 0 & 0$$

REFERENCES

- [1] S. Jajodia and M. Albanese, "An Integrated Framework for Cyber Situation Awareness". Springer International Publishing, 2017, pp. 29–46.
- [2] D. S. Fava, S. R. Byers, and S. J. Yang, "Projecting cyberattacks through variable-length Markov models," *IEEE Transactions on Information Forensics and Security*, vol. 3, no. 3, pp. 359–369, 2008.
- [3] Wikipedia, "December 2015 ukraine power grid cyberattack," 2015, accessed: 2017-10-21.
- [4] CNET, "Wannacry ransomware: Everything you need to know," 2017, accessed: 2017-10-22.
- [5] Washingtonpost, "Massive cyberattack hits europe with widespread ransom demands," 2017, accessed: 2017-10-22.
- [6] S. Smith, "Cybercrime will cost businesses over 2 trillion by 2019," 2015.
- [7] N. Luktarhan, X. Jia, L. Hu, and N. Xie, "Multi-stage attack detection algorithm based on hidden markov model," in *International Conference on Web Information Systems and Mining*. Springer, 2012, pp. 275–282.
- [8] J. Navarro, A. Deruyver, and P. Parrend, "A systematic survey on multi-step attack detection," *Computers & Security*, 2018.
- [9] X. Qin and W. Lee, "Attack plan recognition and prediction using causal networks," in 20th Annual Computer Security Applications Conference, 2004, pp. 370–379.
- [10] F. Valeur, G. Vigna, C. Kruegel, and R. A. Kemmerer, "Comprehensive approach to intrusion detection alert correlation," *IEEE Transactions on Dependable and Secure Computing*, vol. 1, no. 3, pp. 146–169, July 2004.

- [11] B. C. Cheng, G. T. Liao, C. C. Huang, and M. T. Yu, "A novel probabilistic matching algorithm for multi-stage attack forecasts," *IEEE Journal on Selected Areas in Communications*, vol. 29, no. 7, pp. 1438–1448, 2011.
- [12] L. Wang, A. Liu, and S. Jajodia, "Using attack graphs for correlating, hypothesizing, and predicting intrusion alerts," *Computer Communications*, vol. 29, no. 15, pp. 2917 2933, 2006, computer Communications. [Online]. Available: http://www.sciencedirect.com/science/article/pii/S014036640600137X
- [13] H. Du, D. F. Liu, J. Holsopple, and S. J. Yang, "Toward ensemble characterization and projection of multistage cyber attacks," *Proceedings International Conference on Computer Communications and Networks, ICCCN*, 2010.
- [14] A. A. Ramaki, M. Amini, and R. Ebrahimi Atani, "RTECA: Real time episode correlation algorithm for multi-step attack scenarios detection," *Computers and Security*, vol. 49, pp. 206–219, 2015. [Online]. Available: http://dx.doi.org/10.1016/j.cose.2014.10.006
- [15] F. Manganiello, M. Marchetti, and M. Colajanni, "Multistep attack detection and alert correlation in intrusion detection systems," in *Information Security and Assurance*, T.-h. Kim, H. Adeli, R. J. Robles, and M. Balitanas, Eds. Berlin, Heidelberg: Springer Berlin Heidelberg, 2011, pp. 101–110.
- [16] P. Ning and D. Xu, "Learning attack strategies from intrusion alerts," in *Proceedings of the 10th ACM Conference on Computer and Communications Security*, ser. CCS '03. New York, NY, USA: ACM, 2003, pp. 200–209. [Online]. Available: http://doi.acm.org/10.1145/948109.948137
- [17] L. Huiying, P. Wu, W. Ruimei *et al.*, "A real-time network threat recognition and assessment method based on association analysis of time and space," *Journal of Computer Research and Development*, vol. 51, no. 5, pp. 1039–1049, 2014.
- [18] C. Onwubiko, "Situational Awareness in Computer Network Defense: Principles, Methods and Applications". IGI Global, 2012.
- [19] Z. Zali, M. R. Hashemi, and H. Saidi, "Real-time attack scenario detection via intrusion detection alert correlation," in *Information Security and Cryptology (ISCISC)*, 2012 9th International ISC Conference on. IEEE, 2012, pp. 95–102.
- [20] F. Alserhani, M. Akhlaq, I. U. Awan, A. J. Cullen, and P. Mirchandani, "Mars: multi-stage attack recognition system," in Advanced Information Networking and Applications (AINA), 2010 24th IEEE International Conference on. IEEE, 2010, pp. 753–759.
- [21] W. J. Zhang Hengwei, Yang Haopu and L. Tao, "Multi-step attack-oriented assessment of network security situation," *International Journal of Security and Its Application*, vol. 11, no. 1, pp. 203–218, 2017.
- [22] D. Ourston, S. Matzner, W. Stump, and B. Hopkins, "Applications of Hidden Markov Models to Detecting Multi-Stage Network Attacks," *Proceedings of the 36th Annual Hawaiian International Conference on System Sciences*, p. 334, 2003.
- [23] A. Årnes, K. Sallhammar, K. Haslum, T. Brekne, M. E. G. Moe, and S. J. Knapskog, "Real-time risk assessment with network sensors and intrusion detection systems," in *International Conference on Computational and Information Science*. Springer, 2005, pp. 388–397.
- [24] K. Haslum, A. Abraham, and S. Knapskog, "Fuzzy online risk assessment for distributed intrusion prediction and prevention systems," *Proceedings - UKSim 10th International Conference on Computer Modelling and Simulation*, EUROSIM/UKSim2008, pp. 216–223, 2008.
- [25] H. Farhadi, M. Amirhaeri, and M. Khansari, "Alert Correlation and Prediction Using Data Mining and HMM," *The ISC Int'l Journal of Information Security*, vol. 3, pp. 77–101, 2011.
- [26] A. S. Sendi, M. Dagenais, M. Jabbarifar, and M. Couture, "Real time intrusion prediction based on optimized alerts with hidden markov model." *JNW*, vol. 7, no. 2, pp. 311–321, 2012.
- [27] S. Zonouz, K. M. Rogers, R. Berthier, R. B. Bobba, W. H. Sanders, and T. J. Overbye, "Scpse: Security-oriented cyber-physical state estimation for power grid critical infrastructures," *IEEE Transactions on Smart Grid*, vol. 3, no. 4, pp. 1790–1799, 2012.

- [28] H. A. Kholidy, A. Erradi, S. Abdelwahed, and A. Azab, "A finite state hidden markov model for predicting multistage attacks in cloud systems," in *Dependable, Autonomic and Secure Computing (DASC), 2014 IEEE 12th International Conference on.* IEEE, 2014, pp. 14–19.
- [29] U. S. K. Thanthrige, J. Samarabandu, and X. Wang, "Intrusion alert prediction using a hidden markov model," *arXiv* preprint arXiv:1610.07276, 2016.
- [30] P. Holgado, V. A. VILLAGRA, and L. Vazquez, "Real-time multistep attack prediction based on hidden markov models," *IEEE Transactions on Dependable and Secure Computing*, 2017.
- [31] A. R. Ali, R. Abbas, and J. J. Abbas, "A systematic review on intrusion detection based on the hidden markov model," *Statistical Analysis and Data Mining: The ASA Data Science Journal*, vol. 11, no. 3, pp. 111–134, 2018. [Online]. Available: https://onlinelibrary.wiley.com/doi/abs/10.1002/sam.11377
- [32] M. Albanese, S. Jajodia, A. Pugliese, and V. S. Subrahmanian, "Scalable analysis of attack scenarios," *Lecture Notes in Computer Science (including subseries Lecture Notes in Artificial Intelligence and Lecture Notes in Bioinformatics)*, vol. 6879 LNCS, pp. 416–433, 2011.
- [33] L. R. Rabiner, "A tutorial on hidden markov models and selected applications in speech recognition," *Proceedings of the IEEE*, vol. 77, no. 2, pp. 257–286, 1989.
- [34] Snort, "The snort intrusion detection system," 2015.
- [35] Barnyard2, "Barnyard2: an open source interpreter for snort output files," 2016.
- [36] B. Babcock, S. Babu, M. Datar, R. Motwani, and J. Widom, "Models and issues in data stream systems," in *Proceedings of the Twenty-first ACM SIGMOD-SIGACT-SIGART Symposium on Principles of Database Systems*, ser. PODS '02. New York, NY, USA: ACM, 2002, pp. 1–16. [Online]. Available: http://doi.acm.org/10.1145/543613.543615
- [37] L. L. M. I. of Technology, "Defense advanced research projects agency dataset (darpa)," 2015.
- [38] D. Curry, "Intrusion detection message exchange format data model and extensible mark-up language (xml) document type definition," *draft-ietf-idwg-idmef-xml-09. txt*, 2002.
- [39] I. I. D. W. Group et al., "Intrusion detection message exchange format," 2002.
- [40] M. Inc., "Matlab and statistics/ machine learning toolbox release 2014b, natick, massachusetts, united states." 2018.